Hybrid Active Filter for Reactive and Harmonics Compensation in a Distribution Network

Victor Fabián Corasaniti, *Member, IEEE*, Maria Beatriz Barbieri, *Senior Member, IEEE*, Patricia Liliana Arnera, *Senior Member, IEEE*, and María Inés Valla, *Senior Member, IEEE*

***Abstract*—The problem of reactive power and harmonics in the medium voltage level of a power distribution system is considered in this paper. Reconfiguration of the power delivery network imposes new constraints in a distribution substation so that the reactive compensation should be increased. The alternative of a shunt hybrid active filter connected to the 13.8-kV level to enhance the power quality is analyzed in this paper. This proposal uses the existing capacitor bank to build a hybrid filter in which the complementary compensation is performed by the active filter. The performance of the hybrid filter is evaluated with extensive simulations considering reactive power, harmonics, and unbalance compensation. It shows very good behavior in steady-state and transient conditions.**

***Index Terms*—Active filters, harmonic distortion, power distribution, power quality, reactive power.**

I. Introduction

THE INCREASE of nonlinear loads and equipment, as well as the distributed generation units in the power systems, has been demanding the compensation of disturbances caused by them [1], [2]. Voltage distortion, due to current harmonics, has become a major problem for the utilities at distribution levels. Utilities frequently encounter harmonic-related problems, such as higher transformer and line losses, reactive power and resonance problems, derating of distribution equipment, harmonic interactions between the utility and loads, reduced system stability, and reduced safe operating margins [3].

The use of traditional compensation with capacitor banks and passive filters (PFs) gives rise to harmonic propagation, i.e., harmonic voltage amplification due to resonances between line inductances and shunt capacitors. Therefore, active solutions have been continuously analyzed in the last few years [4]–[9].

One of the most popular topologies employed in harmonic compensation is the shunt active power filter (SAPF) [4], [5], [9]. It basically functions as a harmonic current generator feeding the needed harmonics and/or reactive currents at a certain point of the network. Several control strategies have been proposed for the SAPF [6]–[9], and those based on the generalized theory of the instantaneous active and reactive power have been the most popular [10], [11].

The particular problem of a power distribution network is considered in this paper. Reconfiguration of the network imposes new constraints on different distribution substations (DSs). Harmonics studies were performed considering the future configuration of the network. Voltage distortions in different points of the network and the working conditions of the capacitor banks were verified by means of harmonic flows [12]. A first proposal suggested increasing the existing passive compensation, but this solution introduced resonances near the fifth and seventh harmonics resulting in unacceptable distortion levels. Therefore, the alternative of an active compensation was first presented in [13]. A more accurate study of the distribution system modifies the power levels to be compensated and shows that no zero-sequence component was present and that there was very little problem of negative-sequence fundamental currents. The 132-kV voltage system feeding the substation presents almost no harmonics or unbalances. Therefore, it appears as an ideal case to be compensated with shunt active or hybrid filters. A hybrid active filter solution is proposed in this paper. Then, it is extensively evaluated with simulations in steady state as well as transient conditions.

II. Network Description

The 132-kV network, where the DS under study is connected, works meshed and connected to a 500-kV high-voltage transmission system. In the future, the requirement to enhance the voltage profile at 13.8-kV level demands for new compensation [12]. The loads of the different substations are mainly commercial and residential, so it is more difficult to identify the harmonic sources than in the case of industrial plants. Then, it is necessary to build a model based on the field measurements.

Fig. 1 shows the one line diagram of the system model adopted for the DS under test. A digital three-phase model of the network is constructed using the MATLAB/Simulink Power System Blockset (PSB).

The system is represented as an ideal voltage source of 132 kV connected to three transformers of similar characteristics, 132/34.5/13.8 kV and 15/10/15 MVA. The system is modeled by its equivalent impedance related to short circuit power at 13.8 kV, which is approximately 200 MVA. There are

Manuscript received February 14, 2008; revised September 24, 2008. First published October 31, 2008; current version published February 27, 2009. This work was supported in part by the Instituto de Investigaciones Tecnológicas para Redes y Equipos Eléctricos, Facultad de Ingeniería, Universidad Nacional de La Plata (UNLP), in part by the FONCyT-ANPCyT, and in part by the Consejo Nacional de Investigaciones Científicas y Técnicas (CONICET).

V. F. Corasaniti, M. B. Barbieri, and P. L. Arnera are with the Instituto de Investigaciones Tecnológicas para Redes y Equipos Eléctricos–Laboratorios de Alta Tensión, Facultad de Ingeniería, Universidad Nacional de La Plata, 1900 La Plata, Argentina (e-mail: iitree@iitree-unlp.org.ar).

M. I. Valla is with Consejo Nacional de Investigaciones Científicas y Técnicas, 1033 Buenos Aires, Argentina, and also with the Laboratorio de Electrónica Industrial, Control e Instrumentación, Área Departamental de Electrotecnia, Facultad de Ingeniería Universidad Nacional de La Plata, 1900 La Plata, Argentina (e-mail: m.i.valla@ieee.org).

Digital Object Identifier 10.1109/TIE.2008.2007997

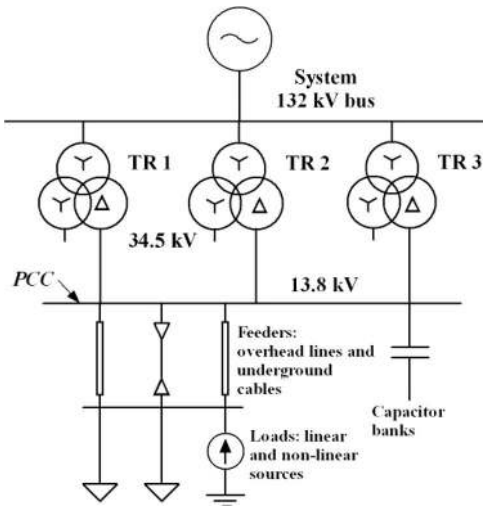

Fig. 1. One-line diagram of system model.

TABLE I
HARMONICS CURRENTS

i_h	i_5 (A)	i_7 (A)	i_{11} (A)	i_{13} (A)	THD_I (%)
Peak values	74.9	54	24.5	18.7	5.4

no loads at the 34.5-kV level. All transformers are connected in parallel to 13.8 kV where the capacitor banks and the loads are placed. Due to the transformer winding connection, Wye/Wye/Delta (Y/Y/D), there are no zero-sequence registers at the 13.8-kV level. In addition, the measurements performed on the network have shown that the load currents present no negative-sequence fundamental component. Then, a balance model network is built for the DS under study. Feeders, underground cables and overhead lines, are considered at the load connection.

The active and reactive power demand at the fundamental frequency is represented by a constant impedance model and the nonlinear load, corresponding to harmonics, through sinusoidal current sources. Their amplitude and frequency correspond to those of each harmonic.

Based on the power flow and harmonics studies performed on the system [12], the power total demand at the 13.8-kV bus is 29.3 MVA with $\cos\varphi = 0.8$. The harmonic peak currents and the THD_I defined in [14] are shown in Table I.

A reactive compensation of 9.6 MVAr will result in $\cos\varphi = 0.94$ at 13.8-kV level, which is the goal for the proposed compensator.

Compensation of the reactive currents with capacitor banks of 4.8 MVAr gives rise to parallel resonances which increase the harmonics to unacceptable levels. The results of this compensation, P and Q defined in [14], together with the reactive power provided by capacitor banks $(Q_{\rm AC})$ and the current and voltage distortion, are summarized in Table II.

Table III summarizes the harmonic voltages and THD_V for all cases, together with the limits fixed by IEEE [15]. For $Q_{\rm C} = 4.8$ MVAr and $Q_{\rm C} = 9.6$ MVAr cases, the individual harmonic voltages for the fifth and the seventh harmonics and THD_V are above the allowable levels, so a different compensation should be considered.

TABLE II
POWERS AND POWER FACTOR RESULTS

Q_c (MVAr)	P (MW)	Q (MVAr)	$V_{1\ phase}$ (kV rms)	THD_v (%)	$I_{1\ line}$ (A rms)	THD_I (%)	$cos\varphi$	Q_{Ac} (MVAr)
0	23.4	17.7	7696	5.66	1269	5.43	0.8	-----
4.8	24.4	13.7	7865	9.65	1188	10.7	0.86	4.78
9.6	25.5	9.7	8040	9.64	1129	13.8	0.92	9.62

TABLE III
VOLTAGE HARMONICS RESULTS AND VERIFICATIONS

Harmonic Voltages	Q_c (0 MVAr)	Q_c (4.8 MVAr)	Q_c (9.6 MVAr)	IEEE limits
V_5 (%)	**3.29**	**5.47**	**8.88**	3
V_7 (%)	**3.32**	**7.48**	**3.61**	3
V_{11} (%)	2.37	2.30	0.86	3
V_{13} (%)	2.14	1.42	0.56	3
THD_V (%)	**5.66**	**9.65**	**9.64**	5

III. HYBRID ACTIVE FILTER COMPENSATION

One of the most popular solutions employed in harmonic compensation, the SAPF, was first presented in [13] as a possible solution to the present problem. Here, a hybrid active filter solution is analyzed in detail. This solution takes advantage of the capacitor bank already installed in the DS under study. The capacitor bank is modified to make a PF. A general structure of the shunt hybrid active power filter (SAPF) is shown in Fig. 2 [18], [19].

It is formed by connecting a shunt PF to the general structure of SAPF analyzed in [13]. The main difference lies in the fact that the measured current not only considers the load current but also the current consumed by the PF.

It is well known that SAPF behaves better with loads that can be modeled as current sources. Then, the capacitor bank is modified to make a PF in order not to load the SAPF with a voltage source. Moreover, tuning the PF near the lowest harmonics present at the load guarantees its behavior as a current source and, at the same time, reduces the current required for the active filter.

Then, the whole compensation is shared by the SAPF and the PF. A reactive power of 4.8 MVAr is compensated by the PF, so less fundamental current is provided by the SAPF. It also supplies the harmonics that are not provided by the PF.

The SAPF consists of a three-phase current-controlled voltage-source inverter (CCVSI) connected to the grid through a coupling inductor and a transformer. In addition, a ripple filter is connected after the transformer to derive the high frequencies generated by the inverter commutation. The current references for the CCVSI are generated by the power control block based on the instantaneous active and reactive power theory. The current loops are closed with hysteresis controllers. The dc side of the inverter is built only with a capacitor of proper value, and the active filter can build up and regulate the dc voltage on the capacitor without any external power supply.

The analysis of the SAPF is divided into two main sections: the CCVSI and the control block to obtain the desired currents and maintain the dc voltage of the CCVSI. In addition, the PF design is shown in this section.

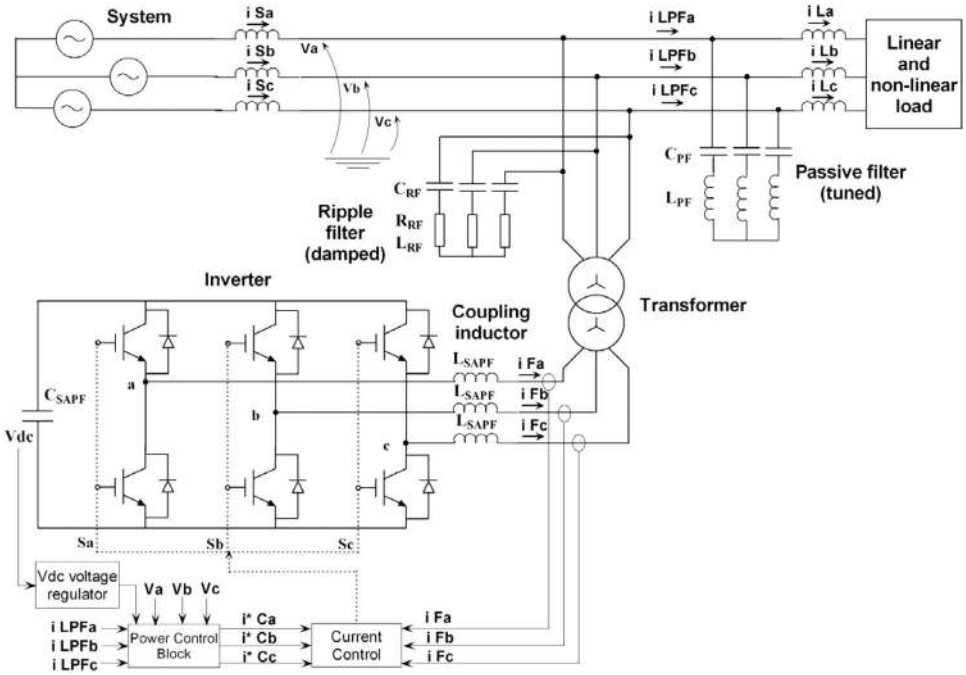

Fig. 2. General structure of the implemented SAPF.

A. Current-Controlled Voltage-Source Inverter

The CCVSI is a standard two-level three-phase voltage-source inverter with IGBTs [1], [16]. The current loops are closed with hysteresis controllers. The output current through the coupling inductor is sampled at a fixed frequency. Therefore, the signal update at the input of the converter is limited to the sampling time, and the maximum value of the switching frequency of the inverter is limited to a value near the sampling frequency. Its mean value is approximately equal to 10 kHz.

The value of the coupling inductor results from a tradeoff between filtering the high frequencies produced by the switching of the converter and allowing high di/dt on the inductor to follow the harmonic currents that should be damped. The switching frequencies are further filtered with a second-order damped parallel filter which takes the high-frequency currents away from the system [3].

The dc side capacitance is selected in order to keep the voltage ripple below 2%. The dc value is chosen so that the converter can supply the current time derivatives demanded by the harmonics to be compensated. The dc voltage level is controlled with a proportional controller which modifies the active power reference to the converter. Although the dc bus capacitor is modeled as a first-order system, its time constant, as well as the dc gain, is defined by the value of the parallel resistance that modeled the dielectric losses of the capacitor. This resistance has several kiloohms, so the dc voltage is almost the integral of the dc current, and a proportional controller is suitable for this situation.

Finally, the coupling transformer adapts the voltage level of the power system (13.8 kV) to ac voltage obtained from the CCVSI with 6.5 kV on the dc side. This transformer provides extra filtering of the switching frequencies.

B. Power Control Block and Reference Current Generator

The power control block mainly measures the network phase voltages (V_a, V_b, V_c) and the phase currents $(i_{\mathrm{LPFa}}, i_{\mathrm{LPFb}}, i_{\mathrm{LPFc}})$ and builds the reference currents for the CCVSI based on the instantaneous active and reactive power theory [10], [11].

First, the measured variables are transformed into the stationary reference frame $[\alpha - \beta - 0]$. Then, instantaneous powers are calculated as

$$\begin{bmatrix} p \\ q \\ p_0 \end{bmatrix} = \begin{bmatrix} p_{\mathrm{DC}} \\ q_{\mathrm{DC}} \\ p_{0\mathrm{DC}} \end{bmatrix} + \begin{bmatrix} p_{0\mathrm{AC}} \\ q_{0\mathrm{AC}} \\ p_{0\mathrm{AC}} \end{bmatrix} = \begin{bmatrix} v_\alpha & v_\beta & 0 \\ -v_\beta & v_\alpha & 0 \\ 0 & 0 & v_0 \end{bmatrix} \cdot \begin{bmatrix} i_\alpha \\ i_\beta \\ i_0 \end{bmatrix} \quad (1)$$

where p is the real power, q is the imaginary power, and p_0 is the zero-sequence power.

The system under study is a three-wire system where the zero sequence may be neglected, so in the sequel, only p and q are considered. In the case of nonlinear loads, p and q have both dc and ac components. The mean value of the instantaneous real power (p_{DC}) equals three times the active power per phase, while the mean value of the instantaneous imaginary power (q_{DC}) equals three times the reactive power per phase. The ac components of both instantaneous powers, (p_{AC}) and (q_{AC}), correspond to the contribution of the harmonics and unbalances. In the present case, the ac components only correspond to harmonics, since there are no unbalance loads and no zero sequence is possible due to the transformer connections.

Generally, the network will supply the dc value of the real power, while its ac component, as well as the whole imaginary power, should be supplied by the SAPF. Then, the instantaneous real power is filtered in order to separate both components and to calculate the reference values p^* and q^*. It is worth noting here that the ac components pass directly to the converter

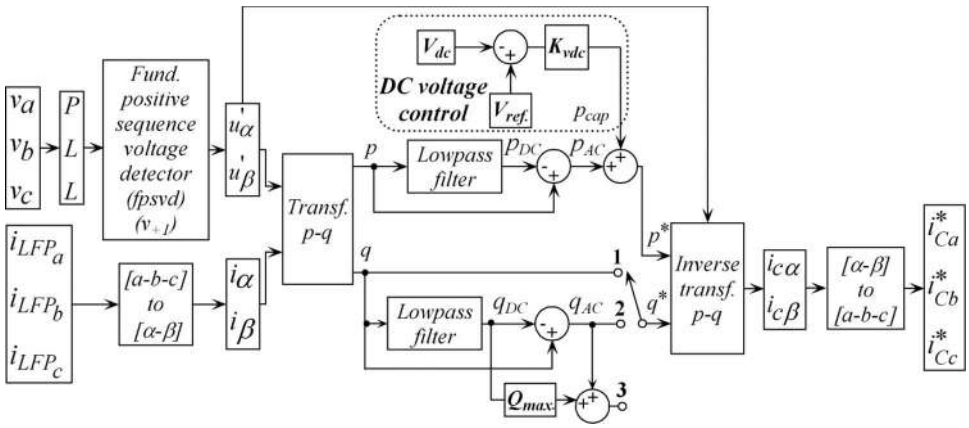

Fig. 3. Power and dc bus control block diagram of the SAPF.

references, so that there is no phase shift. When the ac components may be low, the filter cutoff frequency may affect the transient response but not the phase shift of the ac components of the filter. Then, the reference currents in the $[\alpha-\beta]$ frame are

$$\begin{bmatrix} i_{C\alpha} \\ i_{C\beta} \end{bmatrix} = \frac{1}{v_\alpha^2 + v_\beta^2} \cdot \begin{bmatrix} v_\alpha & v_\beta \\ v_\beta & -v_\alpha \end{bmatrix} \cdot \begin{bmatrix} p^* \\ q^* \end{bmatrix} \tag{2}$$

and the phase currents required for the CCVSI are

$$\begin{bmatrix} i^*_{\mathrm{Ca}} \\ i^*_{\mathrm{Cb}} \\ i^*_{\mathrm{Cc}} \end{bmatrix} = \sqrt{\frac{2}{3}} \cdot \begin{bmatrix} 1 & 0 \\ -1/2 & \sqrt{3}/2 \\ -1/2 & -\sqrt{3}/2 \end{bmatrix} \cdot \begin{bmatrix} i_{C\alpha} \\ i_{C\beta} \end{bmatrix}. \tag{3}$$

The system voltages may be distorted by the harmonic currents as well as the ripple generated by the active filter; therefore, the currents calculated with the previous equation will not exactly compensate the harmonics. Then, it is desirable to obtain the phase angle and frequency of the fundamental positive sequence voltage component (V_{+1}) instead of those directly measured. This is done by a phase-locked loop synchronous with the positive sequence of the sinusoidal phase voltages and a fundamental positive sequence voltage detector (FPSVD) which determines the amplitude of (V_{+1}) [17]. The outputs of the FPSVD are pure sinusoidal phase voltages (V'_a, V'_b, V'_c) which are used to synchronize the filter currents and also to calculate the instantaneous powers.

A complete block diagram of the proposed power control loop is shown in Fig. 3. The active power required for the inverter (p^*) results from the sum of two terms. One corresponds to the ac component of real power (p_{AC}), while the second is the output of the dc-bus voltage control (p_{cap}), which is the power that should be absorbed by the converter to maintain the dc voltage level. Concerning the reference value of q^* selected, there are three possibilities. Option 1 compensates the whole q, which is the mean value (q_{DC}) plus (q_{AC}), option 2 compensates only the ac components of $q(q_{\mathrm{AC}})$, and option 3 compensates the ac components plus a part of the mean value of q determined by the limit $Q_{\max..}$. In this analysis, option 3 is selected with $Q_{\max} = 4.8$ MVAr.

The current control loop of one phase is shown in Fig. 4.

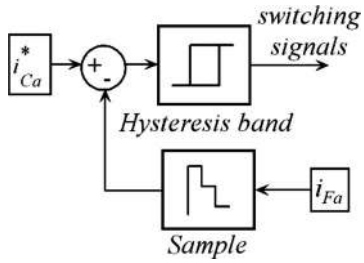

Fig. 4. Current control loop for phase a.

The sampled inverter phase currents $(i_{\mathrm{Fa}}, i_{\mathrm{Fb}}, i_{\mathrm{Fc}})$ are compared, one by one, to the reference currents $(i^*_{\mathrm{Ca}}, i^*_{\mathrm{Cb}}, i^*_{\mathrm{Cc}})$ with three hysteresis comparators, determining the firing signals of the inverter. The inverter currents are sampled at a fixed frequency, so that they are updated to the comparator only at the sampling instants, and the maximum commutation frequency of the inverter is limited to a frequency near the sampling frequency. The hysteresis controller with limited frequency is preferred, since it constitutes a simple, fast, and rugged current control.

C. Passive Filter

The PF consists of simple LC filters per phase that can supply 4.8 MVAr and are tuned near the fifth harmonics [3]. Therefore, defining the reactive power compensation (Q_{CPF}), the tuned harmonic frequency (f_t), and a typical quality factor (Q_{PF}) of PF, the values of C_{PF} (in microfarads), L_{PF} (in millihenries), and R_{PF} (in ohms) are calculated as

$$\begin{aligned} Q_{\mathrm{CPF}}(\mathrm{MVAr}) &= 2 \cdot \pi \cdot f \cdot V^2 \cdot C_{\mathrm{PF}} \\ f_t(\mathrm{Hz}) &= \frac{1}{2 \cdot \pi \cdot \sqrt{L_{\mathrm{PF}} \cdot C_{\mathrm{PF}}}} \\ Q_{\mathrm{PF}} &= \frac{X_o}{R_{\mathrm{PF}}} \end{aligned} \tag{4}$$

where

- f system nominal frequency, 50 Hz;
- V system rms line voltage, 13.8 kV;
- X_{o} inductance (or the capacitance) reactance at resonance (Ω).

TABLE IV
SAPF AND RIPPLE FILTER DESIGN PARAMETERS

Inverter		Transformer		Ripple filter (damped)	
Vdc (V)	6500	S (MVA)	10	R_{RF}(ohm)	30
C_{SHAPF}(uF)	3000	V_1/V_2(kV)	2.3/13.8	C_{RF}(uF)	3.53
L_{SHAPF}(mH)	0.5	X(%)	10	L_{RF}(mH)	3.18
		$L_{2.3kV}$(mH)	0.168	f_c (Hz)	1500

TABLE V
PF DESIGN PARAMETERS

Passive filter (tuned)			
Q_{PF}(MVAr)	4.8	C_{PF}(uF)	80.2
f_1(Hz)	≈ 250	L_{PF}(mH)	5.05
R_{PF}(ohm)	0.17	Q_{PF}	45

TABLE VI
SUMMARY OF COMPONENTS

Components			SAPF	SHAPF
Inverter	IGBT rating	S = √3 /2 .V_{DC}. I_{peak}(MVA)	26	**15**
		Current (A peak)	4600	**2600**
	DC capacitor	Voltage (V)	6500	6500
		C (uF)	7500	**3000**
Coupling inductor			yes	yes
Connection transformer (MVA)			1 x 15	1 x 10
Passive filter (MVAr)			**no**	1 x 4.8
Ripple filter			Yes	Yes

D. Design Parameters

The design parameters of SAPF and the ripple filter are summarized in Table IV, and the PF parameters are in Table V.

Table VI summarizes a comparison between the SAPF proposed here and the SAPF presented and analyzed in [13].

Both filters are designed to compensate the DS presented in this paper. The table clearly shows that the hybrid solution reduces the current rating of the inverter as well as the power level of the connection transformer. As a consequence, the dc bus capacitor may have less capacitance. The hybrid solution is more economical than the active one, particularly considering that the capacitors of the PF are already in the system.

IV. COMPENSATION EVALUATION

In this section, the results from simulations of the SAPF topology, using MATLAB/Simulink PSB, are presented. In order to evaluate the performance of the proposed filter, the DS under study is simulated for different load conditions.

A. Full Load

First, a maximum demand is considered. This means 29.3 MVA with $\cos\varphi = 0.8$ ($P = 23.4$ MW; $Q = 17.7$ MVAr). The voltage and current of one phase at the 13.8-kV level upstream the PF and SAPF are shown in Fig. 5.

The PF is always connected. The SAPF was connected at $t = 0.2$ s. Fig. 5 shows how the distorted currents (dotted line) became sinusoidal and almost in phase with the voltage (solid line), after the SAPF was connected. It also shows that a small high-frequency ripple appears in the phase voltages.

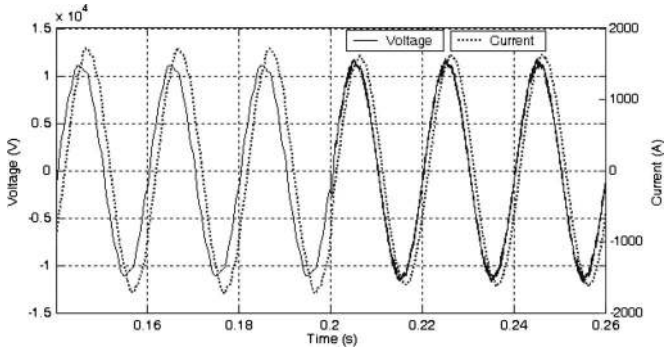

Fig. 5. Full load. Voltage and current in 13.8-kV bus when connecting SAPF.

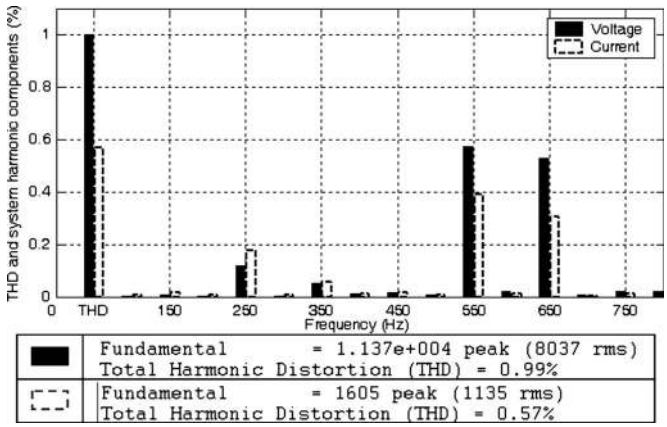

Fig. 6. Full load. Voltage and current THDs and spectra in 13.8-kV bus at steady state.

Fig. 6 shows the phase voltage and line current harmonics spectra. These results correspond to the steady state of full load and a reactive compensation of 9.6 MVAr. The THD_V has been reduced from the original 9.64% to 0.99% in the voltage with a fundamental rms value of $V_{1\text{rms}} = 8037$ V. Regarding current harmonics, the THD_I has been reduced from the original 13.8% to 0.57% with a fundamental rms value of $I_{1\text{rms}} = 1135$ A. Both THD_V and THD_I have been calculated considering up to the 50th order harmonics. When the harmonic order is increased up to 12 kHz, in order to consider the commutation frequency, the THD_V increases to 1.34%, while the current distortions remain almost the same.

B. Unbalanced Load

In this section, the effects of load current unbalances are evaluated. Although there were no problems of system unbalances detected with the previous measurements, some simulations were developed to evaluate the behavior of the filter in presence of negative-sequence fundamental load currents. Here, certain unbalanced load is characterized by a 7% negative-sequence load current (ratio of negative-sequence current to positive sequence current) added to the reactive and harmonics shown in the previous section.

The voltage and current of each phase at the 13.8-kV level upstream the PF and SAPF are shown in Figs. 7 and 8.

The PF is always connected. The SAPF was connected at $t = 0.2$ s. Fig. 7 shows how the distorted voltages in each

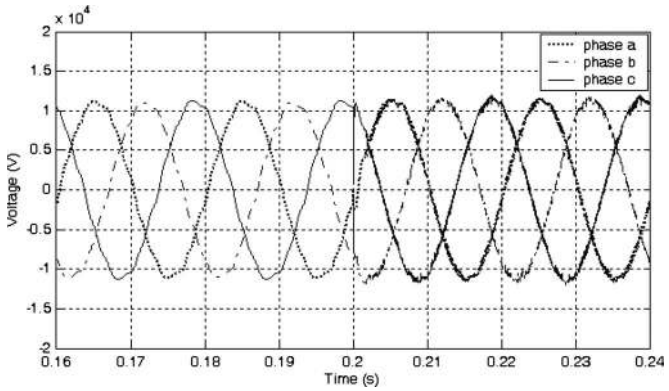

Fig. 7. Unbalanced load. Phase voltages in 13.8-kV bus when connecting SAPF.

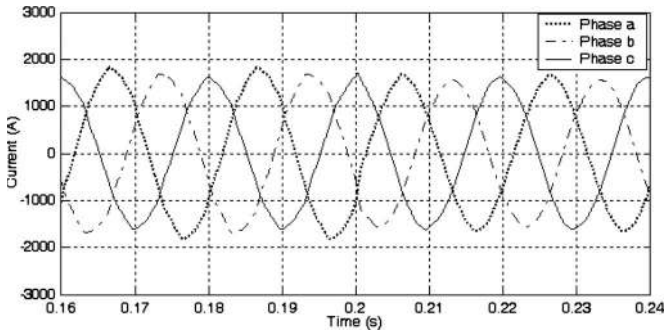

Fig. 8. Unbalanced load. Phase currents in 13.8-kV bus when connecting SAPF.

phase became sinusoidal, after the SAPF was connected. It also shows that a small high-frequency ripple appears in the phase voltages. The original voltage unbalance of 1% was reduced to 0.26% with the control of the active filter. Fig. 8 shows how the distorted and unbalanced currents in each phase became sinusoidal and with low unbalance, after the SAPF was connected. The negative sequence of 7% originally considered was reduced to 2%.

Fig. 9 shows the phase voltage and line current harmonics. These results correspond to the steady state of full load and a reactive compensation of 9.6 MVAr. The THD_V has been kept below 1.3% with a fundamental rms value of $V_{1\text{rms}} = 8029$ V. Regarding current harmonics, the THD_I has been kept below 1.8% with a fundamental rms value of $I_{1\text{rms}} = 1143$ A. Both THD_V and THD_I have been calculated considering up to 50th order harmonics. When the harmonic order is increased up to 12 kHz, to consider the commutation frequency, the THD_V increases to 2.3%, while the current distortions remain almost the same. It is worth noting that the voltage and current distortion increments are mainly due to a third positive-sequence harmonic generated by the fundamental negative-sequence current and a second harmonics dc voltage ripple.

C. Load Change

First, the load and distortion corresponding to the 50% of maximum demand are considered at the 13.8-kV bus. Voltage and current of one phase at the 13.8-kV level upstream the SAPF are shown in Fig. 10.

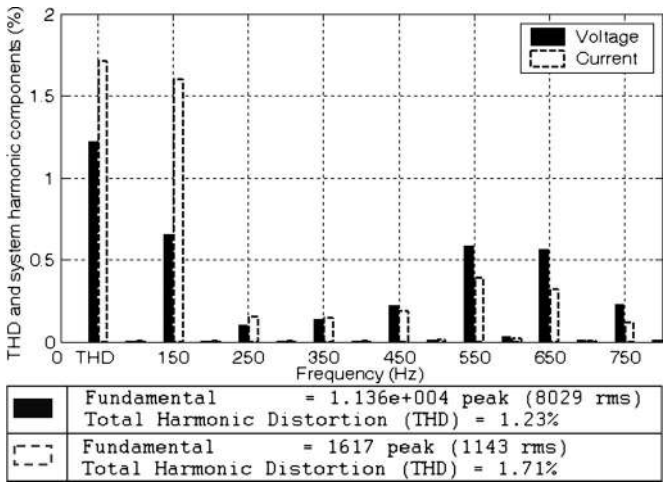

Fig. 9. Unbalanced load. Voltage and current THDs and spectra in 13.8-kV bus at steady state.

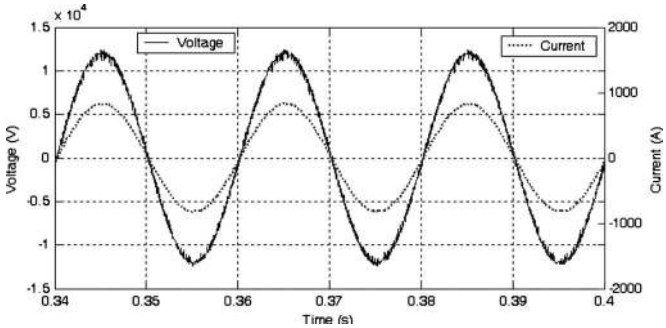

Fig. 10. 50% of full load. Voltage and current in 13.8 kV at steady state.

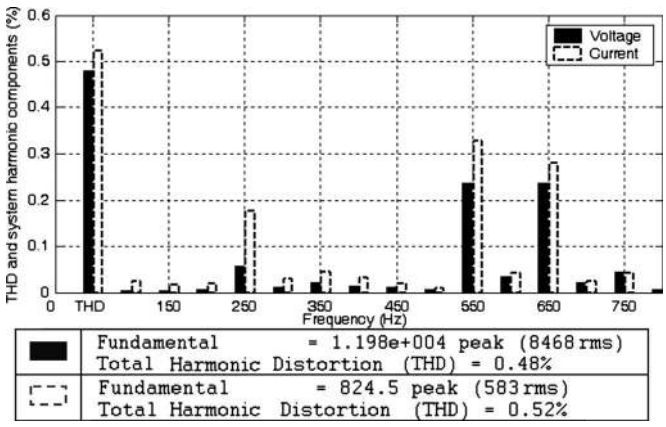

Fig. 11. 50% of full load. Voltage and current THDs and spectra in 13.8 kV at steady state.

The THD_V, THD_I, and the individual harmonics of phase voltage and line current, corresponding to the steady state with 50% of full load and a reactive compensation of 9.6 MVAr, are shown in Fig. 11. They are presented in [%] of their fundamental values. THD_V results 0.48%, and THD_I results 0.52%. When the harmonic order is increased up to 12 kHz, to consider the commutation frequency, the THD_V increases to 1.03%, while the current distortions remain almost the same.

At $t = 0.4$ s, the load is increased to its maximum demand. The PF and SAPF are already connected. Voltage and current

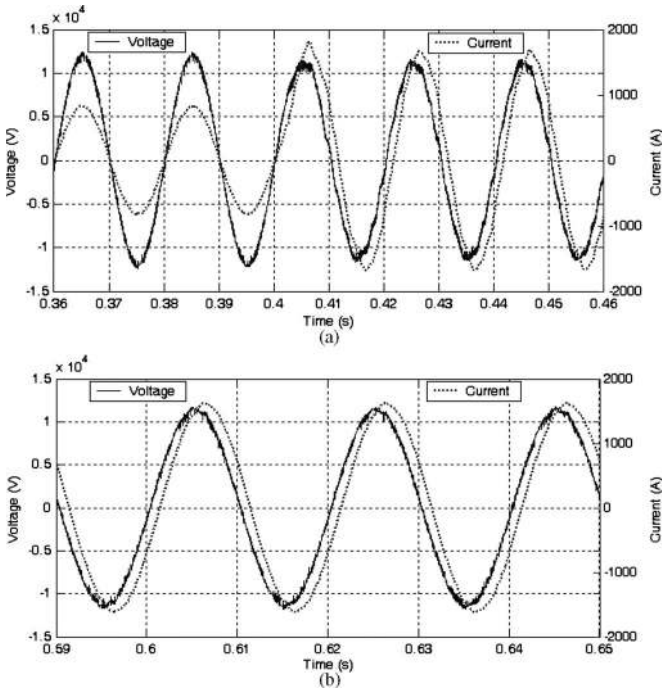

Fig. 12. Load increase from 50% to 100%. Voltage and current in 13.8-kV bus. (a) Load transients. (b) Steady state.

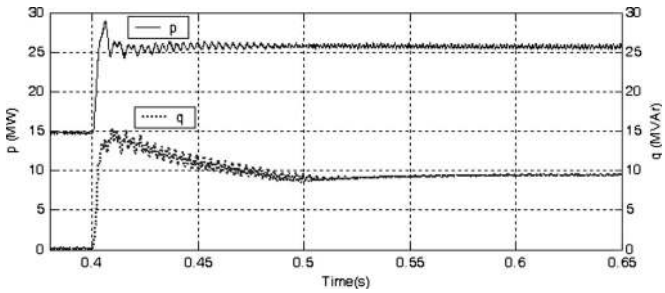

Fig. 13. Real and imaginary power in 13.8 kV when the load increase is from 50% to 100%.

of one phase at the 13.8-kV level upstream the PF and SAPF when the load is increased are shown in Fig. 12.

Fig. 12(a) shows a transient in line voltage and current after the increment of the load. The amplitude of the current in the system increases due to the raise of the load. The amplitude of the voltage decays because the value of the reactive power compensation of the SAPF continues being the same ($Q_{\rm C} = 9.6$ MVAr). The distortions in the current and the voltage increase during the transients. Fig. 12(b) shows that the SAPF fully compensates the harmonic distortion after the transient.

Fig. 13 shows the transients of powers at 13.8-kV bus. The reactive compensation is shown in the imaginary power (lower trace). At $t = 0.4$ s, the active and reactive power increases from 50% to the full load. After a transient of 100 ms, the dc component of the imaginary power corresponds to the full load minus 9.6 MVAr of reactive compensation supplied by the SAPF. Its ac component is almost cancelled by the SAPF.

The performance of the CCVSI is shown in Fig. 14, showing the current delivered by the converter and the dc voltage when load changes from 50% to 100%. The upper trace shows the

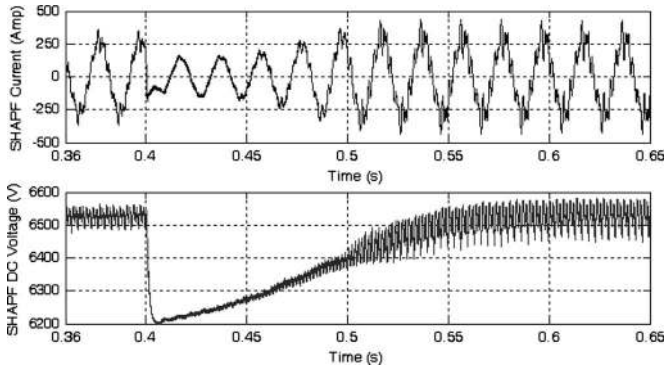

Fig. 14. Load change. Current into the PCC and dc voltage of the CCVSI.

TABLE VII
POWERS AND POWER FACTOR RESULTS

Case	Q_c (MVAr)	P (MW)	Q (MVAr)	V_{1phase} (kV rms)	THD_v (%)	$I_{1\ line}$ (A rms)	THD_I (%)	$cos\varphi$
Balance	9.6	25.7	9.45	8037	0.99	1135	0.57	0.94
Unbalance	9.6	25.65	9.16	8029	1.23	1143	1.71	0.94

TABLE VIII
VOLTAGE HARMONICS RESULTS AND VERIFICATIONS

Harmonic voltages	Q_c (9.6 MVAr)		IEEE limits
	balance	unbalance	
V_3 (%)	0	0.63	3
V_5 (%)	0.12	0.11	3
V_7 (%)	0.05	0.12	3
V_9 (%)	0	0.23	3
V_{11} (%)	0.58	0.59	3
V_{13} (%)	0.53	0.57	3
THD_V (%)	0.99	1.23	5

current of one phase entering the PCC. Its fundamental value corresponds to 4.8 MVAr of reactive compensation, while the harmonics are those of the load minus those damped by the tuned PF. The bottom trace shows that the dc voltage suffers a voltage drop of around 5% when the load is increased from 50% to 100% ($t = 0.4$ s), but it reestablishes its mean value in 150 ms. It presents a 12th harmonics oscillation due to the ac component of the instantaneous active power. In this case, the 5th and 7th harmonics are mostly damped by the PF, so 11th and 13th dominate the voltage ripple.

The results of SAPF compensation at the 13.8-kV bus system are summarized in Table VII.

Table VIII summarizes the harmonic voltages and THD_V with the SAPF compensation together with the limits fixed by IEEE [15]. The individual harmonic voltages and THD_V are well below the allowable levels.

V. CONCLUSION

The design of a hybrid active filter to compensate reactive power, harmonics, and unbalance loads in the medium voltage level of a power distribution system was presented in this paper. This solution used the existing capacitor bank and built the complementary compensation with the active filter. The capacitor bank was modified to make a tuned filter near the fifth harmonics. The proposal shows very good performance

and may be more economical than a shunt active filter solution since it uses capacitors already present in the system and results in a lower rating inverter.

The proposed SAPF is a very good solution for power systems in which the voltage generation is almost ideal and the loads present little unbalance. Compensation of distorted and unbalance voltage systems will require more complex solutions like the universal power quality controller.

REFERENCES

[1] E. Acha, V. G. Agelidis, O. Anaya-Lara, and T. J. E. Millerin, *Power Electronic Control in Electrical Systems* (Newnes Power Engineering Series). Shropshire, U.K.: Newnes, 2002.

[2] F. Blaabjerg, R. Teodorescu, M. Liserre, and A. V. Timbus, "Overview of control and grid synchronization for distributed power generation systems," *IEEE Trans. Ind. Electron.*, vol. 53, no. 5, pp. 1398–1409, Oct. 2006.

[3] J. Arrillaga and N. R. Watson, *Power System Harmonics*, 2nd ed. Hoboken, NJ: Wiley, 2003.

[4] H. Akagi, "Active harmonic filters," *Proc. IEEE*, vol. 93, no. 12, pp. 2128–2141, Dec. 2005.

[5] B. Singh, K. Al-Haddad, and A. Chandra, "A review of active filters for power quality improvement," *IEEE Trans. Ind. Electron.*, vol. 46, no. 5, pp. 960–971, Oct. 1999.

[6] B. Singh, V. Verma, and J. Solanki, "Neural network-based selective compensation of current quality problems in distribution system," *IEEE Trans. Ind. Electron.*, vol. 54, no. 1, pp. 53–60, Feb. 2007.

[7] D. O. Abdeslam, P. Wira, J. Merckle, D. Flieller, and Y. Chapuis, "A unified artificial neural network architecture for active power filters," *IEEE Trans. Ind. Electron.*, vol. 54, no. 1, pp. 61–76, Feb. 2007.

[8] B. R. Lin and C. H. Huang, "Implementation of a three-phase capacitor-clamped active power filter under unbalanced condition," *IEEE Trans. Ind. Electron.*, vol. 53, no. 5, pp. 1621–1630, Oct. 2006.

[9] K. K. Shyu, M. Yang, Y. M. Chen, and Y. F. Lin, "Model reference adaptive control design for a shunt active-power-filter systems," *IEEE Trans. Ind. Electron.*, vol. 55, no. 1, pp. 97–106, Jan. 2008.

[10] H. Akagi, E. Watanabe, and M. Aredes, *Instantaneous Power Theory and Applications to Power Conditioning* (IEEE Press Series on Power Engineering). New York: Wiley, 2007.

[11] R. S. Herrera, P. Salmerýn, and H. Kim, "Instantaneous reactive power theory applied to active power filter compensation: Different approaches, assessment, and experimental results," *IEEE Trans. Ind. Electron.*, vol. 55, no. 1, pp. 184–196, Jan. 2008.

[12] V. F. Corasaniti, M. B. Barbieri, P. L. Arnera, and M. I. Valla, "Load characterization in medium voltage of an electric distribution utility related to active filters," in *Proc. IEEE PES Transmiss. Distrib. Conf.—Exposition Latin America*, Caracas, Venezuela, Aug. 2006, pp. 1–7.

[13] V. F. Corasaniti, M. B. Barbieri, P. L. Arnera, and M. I. Valla, "Reactive and harmonics compensation in a medium voltage distribution network with active filters," in *Proc. IEEE ISIE*, Vigo, Spain, Jun. 2007, pp. 2510–2515.

[14] "IEEE PES special publication of 'Tutorial on harmonics modeling and simulation'," 1998. IEEE Catalog Number: 98TP125-0.

[15] *Recommended Practices and Requirements for Harmonic Control in Electrical Power Systems*, IEEE Std. 519-1992.

[16] N. G. Hingorani and L. Gyugyi, *Understanding FACTS: Concepts and Technology of Flexible AC Transmission Systems*. Piscataway, NJ: IEEE Press, 1999.

[17] M. Aredes, L. F. C. Monteiro, and J. M. Miguel, "Control strategies for series and shunt active filters," in *Proc. IEEE PowerTech Conf.*, Bologna, Italy, Jun. 2003, vol. 2.

[18] H. Akagi, "New trends in active filters for power conditioning," *IEEE Trans. Ind. Appl.*, vol. 32, no. 6, pp. 1312–1322, Nov./Dec. 1996.

[19] S. Bhattacharya and D. Divan, "Active filter solutions for utility interface of industrial loads," in *Proc. IEEE Int. Conf. Power Electron., Drives Energy Syst. Ind. Growth*, Jan. 1996, vol. 2, pp. 1078–1084.

Victor Fabián Corasaniti (S'05–M'07) received the Electrical Engineer and Master in Engineering degrees from the National University of La Plata (UNLP), La Plata, Argentina, in 1999 and 2008, respectively.

Since 1999, he has been with the Instituto de Investigaciones Tecnológicas para Redes y Equipos Eléctricos–Laboratorios de Alta Tensión, Facultad de Ingeniería, UNLP, studying normal and transient conditions of electrical systems and technical planning. He is also an Assistant Professor with the Electrical Engineering Department, UNLP. His special fields of interest include power system operation and control, power quality, and power electronics.

Maria Beatriz Barbieri (M'97–SM'01) received the degree in telecommunications engineering (with honors) from the National University of La Plata (UNLP), La Plata, Argentina, in 1984.

Since 1983, she has been with the Instituto de Investigaciones Tecnológicas para Redes y Equipos Eléctricos–Laboratorios de Alta Tensión, Facultad de Ingeniería, UNLP, studying normal and transient conditions of electrical systems and economic and technical planning. She is also a Professor of electricity and magnetism with the Electrical Engineering Department, UNLP. Her interests include electrical power systems.

Prof. Barbieri is the Argentina IEEE PES Chapter Chairman.

Patricia Liliana Arnera (M'99–SM'01) received the degree in electrical engineering from the National University of La Plata (UNLP), La Plata, Argentina, in 1981.

She is currently the Head of the Instituto de Investigaciones Tecnológicas para Redes y Equipos Eléctricos–Laboratorios de Alta Tensión, Facultad de Ingeniería (FI), UNLP, studying transient conditions of electrical systems and working in electromagnetic fields and health. She is a Full Professor of power system with the Electrical Engineering Department, FI-UNLP. Her interests include electrical power systems.

Prof. Arnera is a member of the Buenos Aires Academy of Engineering in Argentina. She was the Argentina IEEE PES Chapter Chairman during 2001–2002.

María Inés Valla (S'79–M'80–SM'97) received the Electronics Engineer and Doctor in Engineering degrees from the National University of La Plata (UNLP), La Plata, Argentina, in 1980 and 1994, respectively.

She is currently a member of the Consejo Nacional de Investigaciones Científicas y Técnicas, Buenos Aires, Argentina. She is also currently with the Laboratorio de Electrónica Industrial, Control e Instrumentación, Área Departamental de Electrotecnia, Facultad de Ingeniería, UNLP, where she is also currently a Full Professor with the Electrical Engineering Department. She is engaged in teaching and research on power converters and ac motor drives.

Prof. Valla is a member of the Buenos Aires Academy of Engineering in Argentina. Within IEEE, she is a member of the Ethics and Membership Conduct Committee and a senior member of the Administrative Committee of the IEEE Industrial Electronics Society. She has been a member of the organizing committees of several international conferences.